Uncertainties in Seasonal Wind Torques over the Ocean

Rui M. Ponte, Amala Mahadevan, Jayendran Rajamony, and Richard D. Rosen

Atmospheric and Environmental Research, Inc., Lexington, Massachusetts

ABSTRACT

Changes in axial atmospheric angular momentum M are related to zonal torques on the atmosphere, but studies reveal large imbalances between the estimated torques and M variations on seasonal timescales. The observed imbalances are commonly attributed to uncertainties in the torque estimates. One particularly important torque component at the seasonal period is that due to zonal wind stresses over the ocean T_O. The uncertainties in T_O are explored by calculating different multiyear time series based on surface wind products derived from passive and active microwave satellite data. The satellite-based T_O are compared to available reanalysis products. Results indicate that there are indeed substantial uncertainties in the seasonal T_O, and that these uncertainties are related mostly to the wind fields rather than to the particular parameterizations of the surface stress in the boundary layer. Regional analyses point to the need to improve knowledge of the wind fields over extensive areas of the ocean, particularly in many tropical and southern latitude regions. Resolving subweekly variability in surface winds is also found to be important when determining the seasonal cycle in T_O. The current satellite-based T_O estimates can lead to a better seasonal momentum budget, but results are tempered by the uncertain effects of gravity wave torque in that budget.

1. Introduction

The atmospheric angular momentum M about the polar axis, which includes contributions from both wind and mass signals (Rosen 1993), varies considerably in time. The largest variation occurs at the seasonal timescale and is associated primarily with annual and semiannual oscillations in the zonal winds, especially in the Tropics and subtropics (Rosen et al. 1991; Rosen 1993; Huang and Sardeshmukh 2000). From conservation principles, such seasonal changes in M must result from torques that exchange angular momentum with the solid earth and oceans according to the relation

$$\dot{M} \equiv \frac{dM}{dt} = T_L + T_O, \qquad (1)$$

where T_L and T_O are the torques acting on the atmosphere at the land and ocean interfaces, respectively. Torques over land include the friction torque T_f due to surface wind stresses, the mountain torque T_m due to pressure differences across orography, and the gravity wave torque T_{gw} representing transfers associated with internal wave generation by unresolved small-scale orography (e.g., Boer 1990). For T_O, only frictional effects are relevant.

Studies examining the torques responsible for the sea-

Corresponding author address: Dr. Rui M. Ponte, Atmospheric and Environmental Research, Inc., 131 Hartwell Ave., Lexington, MA 02421-3126.
E-mail: ponte@aer.com

sonal cycle in M date back to White (1949) and Widger (1949) but have been relatively rare, in part due to the lack of appropriate observations (see review by Rosen 1993). More recent attempts include the model studies by Boer (1990) and Lejenäs et al. (1997) and the analyses based on observations by Wahr and Oort (1984), Ponte and Rosen (1993, 2001) and Huang et al. (1999). These studies clarify the importance of the friction torque, in particular its ocean component T_O, in explaining the seasonal cycle in M. Yet, establishing a balance between the torques and $\dot{M}$, as required by (1), has proved difficult with observations. Huang et al. (1999) found large discrepancies in the $\dot{M}$ and torque balance at seasonal timescales when they used 29 yr of the National Centers for Environmental Prediction–National Center for Atmospheric Research (NCEP–NCAR) reanalysis data (see also Ponte and Rosen 2001).

Problems with the $\dot{M}$ and torque balance computed with the NCEP–NCAR dataset are largely attributed to errors in the estimated torques, including possible problems with T_{gw} (Huang et al. 1999). The discrepancies in the seasonal budget are far larger than expected errors in $\dot{M}$ (Ponte and Rosen 2001). In contrast, torques are inherently uncertain owing to the many parameterizations of surface processes needed to calculate them. Estimates of T_O, which depend on knowledge of surface zonal winds, may be particularly prone to large error (e.g., Bryan 1997) because wind observations are very sparse over the ocean. Given the importance of T_O for the seasonal M budget, an assessment of its uncertainties thus seems in order.

Ponte and Rosen (1993) demonstrated that estimates of T_O were significantly altered by the use of surface wind data derived from the Special Sensor Microwave Imager (SSM/I) satellite instruments over the 1987–89 period. Similar results were obtained by Xu (1997) and Salstein et al. (1996) with wind scatterometer data from the first European Remote Sensing satellite (*ERS-1*). Using other torque and M data from NCEP operational analysis and NCEP–NCAR reanalysis, they were also able to show slight improvements in the M balance when using the scatterometer-based T_O values. Since these studies, significantly longer SSM/I and scatterometer datasets have been created. Here we make use of these longer datasets and the NCEP–NCAR torque dataset of Huang et al. (1999) to reexamine the seasonal $\dot{M}$ and torque balance. Our goals are to assess the uncertainty in T_O on seasonal timescales, to identify where the largest errors in T_O lie, and to determine whether the uncertainty in T_O is a significant hurdle toward attaining a closed seasonal M budget. The various T_O products and their calculation, as well as other ancillary torque and M data used, are discussed in section 2, followed by a detailed comparison of the T_O estimates and discussion of their differences in section 3. In section 4, the various T_O estimates are assessed in the context of the seasonal M budget before a summary and final remarks are presented in section 5.

2. Torque and ancillary datasets

Given a zonal wind stress field τ at the atmosphere's lower boundary, the ocean torque on the atmosphere T_O can be calculated as

$$T_O = \int_S a \cos\phi \, \tau \, dS, \tag{2}$$

where a is the earth's radius, ϕ denotes latitude, and S is the surface of the ocean. The sign convention is such that for near-surface eastward winds $\tau < 0$; consequently $T_O < 0$ and acts to decrease M. The calculation of the various different estimates of T_O and related torque and M quantities used in this study is detailed below.

a. NCEP–NCAR reanalysis

Motivation for the present work stems partly from the availability of the comprehensive NCEP–NCAR reanalysis torque and M dataset described by Huang et al. (1999) and Ponte and Rosen (1999). In brief, the data include 6-hourly gridded values of zonal wind on pressure levels up to 10 hPa, surface pressure, and the various torques (T_f, T_m, T_{gw}) on the atmosphere for the period 1958 to the present. Daily values of M, $\dot{M}$, T_L, and T_O, as calculated by Ponte and Rosen (2001), are used here for comparison with the satellite-based estimates of T_O and for analyses of T_O in the context of the

M budget. Full details of all the quantities, including their mathematical definitions and time series plots, are given by Huang et al. (1999) and Ponte and Rosen (1999, 2001).

The spectra of $\dot{M}$ and the total torque $T(=T_L + T_O)$ considered by Ponte and Rosen (2001) exhibit peaks at frequency bands centered at the annual and semiannual periods,[1] along with a clear imbalance between the variance of $\dot{M}$ and T over the same bands. Our analysis focuses therefore on the annual and semiannual cycles. The amplitude and phase of the annual and semiannual harmonics of $\dot{M}$ and T shown in Fig. 1 highlight more clearly the seasonal discrepancies in the M budget. Harmonics were determined by conventional Fourier analysis. The values of T used in Fig. 1 include contributions from T_{gw}; given its uncertain role in the budget (Huang et al. 1999; Ponte and Rosen 2001), results without T_{gw} effects are also considered later in section 4. The imbalance at the annual period is large, mostly because of phase differences between $\dot{M}$ and T. For the semiannual period, amplitude and phase agreement is considerably better. From the values of T_O also plotted in Fig. 1, it is clear that T_O is an important component of T and that possible uncertainties in T_O could play a role in the observed discrepancies between $\dot{M}$ and T.

b. Ocean torque from SSM/I winds

With the idea of enhancing the quality of wind fields provided by operational weather centers, Atlas et al. (1991) pioneered a variational approach in which SSM/I-derived surface wind estimates are merged with the gridded wind fields from the European Centre for Medium-Range Weather Forecasts (ECMWF) to produce satellite-enhanced 6-hourly surface fields on a $1° \times 1°$ global grid. Production of such wind fields has continued (Atlas et al. 1996), and a multiyear dataset spanning the period 1987–99 is now available.

Following Ponte and Rosen (1993), we use the multiyear SSM/I-based wind dataset to calculate T_O based on two different estimates of the wind stress τ. One set of τ values was provided by J. C. Jusem (2000, personal communication) and is based on a complete treatment of boundary layer processes using the model of Liu et al. (1979) and relevant input surface variables from ECMWF. This τ dataset spans only the period 1994–98 because auxiliary input fields were not available for other years. In addition, values for January 1997 are missing; we have used mean January values calculated from the available years to fill in this gap.

We calculated a second set of τ values for the entire

---

[1] Unlike M, most of the variance in $\dot{M}$ is at subseasonal periods (cf. Table 1 in Ponte and Rosen 1993; Fig. 1 in Huang et al. 1999). Thus, although the $\dot{M}$ spectrum shows peaks at the annual and semiannual bands, the seasonal signal is small compared to the total variance in $\dot{M}$. This makes analysis of the seasonal torque balance difficult.
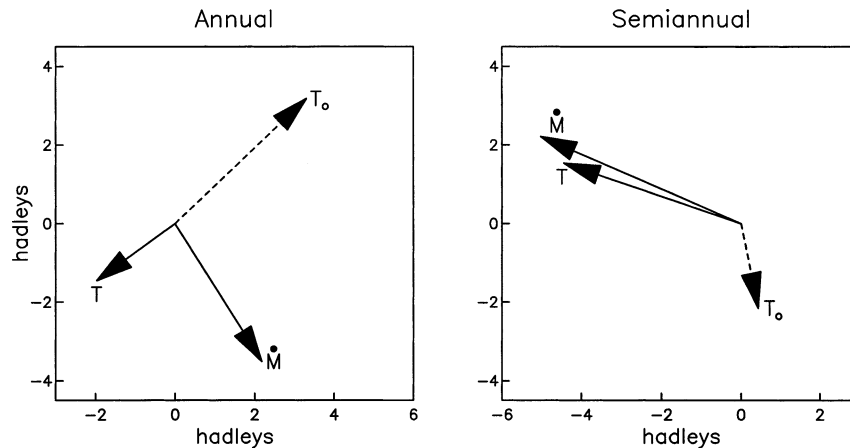
FIG. 1. Annual and semiannual amplitude and phase of $\dot{M}$, T, and T_O, based on NCEP–NCAR reanalysis data for 1968–98, plotted in a phasor diagram, where amplitude and phase are represented by the length and direction of a vector, respectively. Amplitudes are given in units of hadleys (1 hadley $= 10^{18}$ kg m^2 s^{-2}). Phase is plotted increasing counterclockwise, with 90° given by a phasor pointing straight upward. A phase of 0° corresponds to an annual maximum on 1 Jan or semiannual maxima on 1 Jan and ~6 months later.

1987–99 period using the bulk formulation of Large and Pond (1982). In this calculation, the drag coefficient is dependent only on wind speed; dependencies on other parameters like the air–sea temperature difference and relative humidity are neglected. Time series of T_O based on this simple scheme, hereafter denoted as SSMI$_{LP}$ (for Large and Pond), will be later contrasted with the GSFC series, denoted simply as SSMI, for the overlapping period.

c. Ocean torque from scatterometer winds

Data from several scatterometer instruments flown to date [on *ERS-1, ERS-2,* and the NASA scatterometer (NSCAT) on *ADEOS*] have been processed and objectively mapped into weekly 1° × 1° surface wind fields over the global oceans (80°S–80°N) at the Centre ERS d'Archivage et de Traitement (CERSAT) in Brest, France. We have used the data distributed on CD-ROM by CERSAT (2000) to calculate T_O time series based on *ERS-1* and *ERS-2* data. Besides wind speed values, gridded stress data based on the bulk formulation of Smith (1988) are also provided on the CD. We have used these τ values and also τ values computed by us as described in section 2b to calculate two sets of T_O, denoted hereafter as SCAT and SCAT$_{LP}$, respectively.

3. Analysis of T_O

a. How well is T_O known?

For the purposes of comparing different T_O products, it is desirable to use the longest period of overlap available, to obtain as stable an estimate of the annual and semiannual harmonics as possible. To this end, we compare T_O time series from NCEP–NCAR, SSMI$_{LP}$, and SCAT$_{LP}$ for the overlapping 8-yr period from 1992 to 1999. (The first complete year of SCAT$_{LP}$ series is 1992, while the SSMI$_{LP}$ series ends in 1999.) We work with SSMI$_{LP}$ values, based on our simple stress model, because the available SSMI series is only five years long. For consistency, SCAT$_{LP}$ is also used. Dependence of results on the stress model is discussed in section 3b.

Using simple Fourier analysis, we calculate amplitudes and phases of the annual and semiannual cycles for the three time series of T_O (Fig. 2). The 4 times daily T_O values from NCEP–NCAR and SSMI$_{LP}$ series are weekly averaged to be consistent with SCAT$_{LP}$ series before performing the harmonic analysis. Phases of the various T_O estimates in Fig. 2 are all similar but vary over a range of ~5°–30° (annual maxima from late January to early February; semiannual maxima around mid- to late May and six months later). Differences in amplitude are noticeable (~1 or 2 hadleys, where 1 hadley $\equiv 10^{18}$ kg m^2 s^{-2}), with SCAT$_{LP}$ having the smallest values. Uncertainties in the semiannual cycle seem to be bigger than for the annual cycle, relative to their amplitudes. Similar conclusions can be drawn from the 3-month-average values of T_O shown in Fig. 3. The strong annual cycle for SSMI$_{LP}$ comes from larger torques during the northern winter and summer seasons. SCAT$_{LP}$ values are generally the smallest. The estimated range of seasonal variability in Figs. 2 and 3 is not inconsistent with the spread of values that can be inferred from previous calculations of T_O based on observations (Ponte and Rosen 1993, 1994; Bryan 1997) and models (Boer 1990).
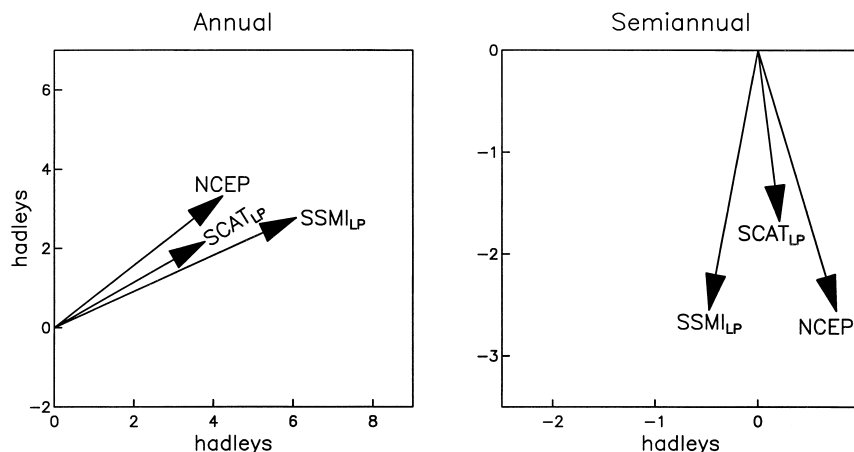
FIG. 2. As in Fig. 1 but for T_O phasors derived from NCEP–NCAR, SSMI$_{LP}$, and SCAT$_{LP}$ series based on the period 1992–99.

b. Sources of uncertainty in T_O

One of the uncertain aspects in the calculation of T_O relates to the many different formulations of the boundary layer model that can be used to convert wind speed to stress τ. Sensitivity to the stress model can be examined by comparing values of T_O based on the same winds but different schemes to estimate τ. Comparisons of SCAT and SCAT$_{LP}$, based on the same scatterometer winds (1992–99), and SSMI and SSMI$_{LP}$, based on the same SSM/I winds (1994–98), can serve this purpose. Annual and semiannual harmonics calculated for these two pairs of T_O time series are shown in Fig. 4.

Although the series in Fig. 4 are calculated using different bulk and boundary layer stress models (see section 2), their amplitudes and phases are very similar for SCAT and SSMI pairs. The largest difference is ∼1 hadley for the annual cycle calculated with the scatterometer data. Differences between SSMI and SSMI$_{LP}$ values are much smaller. In fact, the differences among

T_O values in Fig. 2 are generally larger than the differences between SSMI and SSMI$_{LP}$ or between SCAT and SCAT$_{LP}$ in Fig. 4. Sensitivity of T_O to the stress model is thus small.

The T_O is likely more sensitive to other factors, such as the temporal resolution of the wind fields. The SCAT$_{LP}$ series is based on weekly wind fields, in contrast with the 6-hourly winds used for NCEP–NCAR and SSMI$_{LP}$ series. Because of the nonlinear relation between wind speed and τ, the seasonal cycle in τ can depend on wind variability at periods other than annual and semiannual. Wind variability even at subweekly timescales could be relevant. To assess the effects of temporal resolution of the wind fields on T_O, we calculate another T_O time series (denoted SSMI$'_{LP}$) using weekly averaged SSM/I-based winds as input to the same stress model used for SSMI$_{LP}$. Comparisons of SSMI$_{LP}$ and SSMI$'_{LP}$ annual and semiannual cycles are given in Fig. 5. The estimated vector differences are ∼25% and 50% of the SSMI$_{LP}$ amplitudes for the annual and semiannual terms, respectively. Note also that SSMI$'_{LP}$ results are closer to those of SCAT$_{LP}$ in Fig. 2, suggesting that different time resolutions of the wind fields might help explain part of the SCAT$_{LP}$ and SSMI$_{LP}$ differences noted in Fig. 2. The results in Fig. 5 indicate that it is important to have good knowledge of synoptic, subweekly wind variability when determining the seasonal cycle in τ and consequently T_O.

Differences between SSMI$_{LP}$ and NCEP–NCAR values in Figs. 2 and 3 are not affected by time resolution issues and give a good idea of the sensitivity of T_O to different wind fields, assuming that differences introduced by the stress models are relatively modest (Fig. 4). The quality of the wind fields may be regionally dependent, and regional comparisons of τ fields can indicate where uncertainties in wind and τ fields might be large. Such an analysis is illustrated in Fig. 6 by showing gridded, 3-month-averaged τ fields used to calculate the SSMI$_{LP}$ and NCEP–NCAR series of T_O and
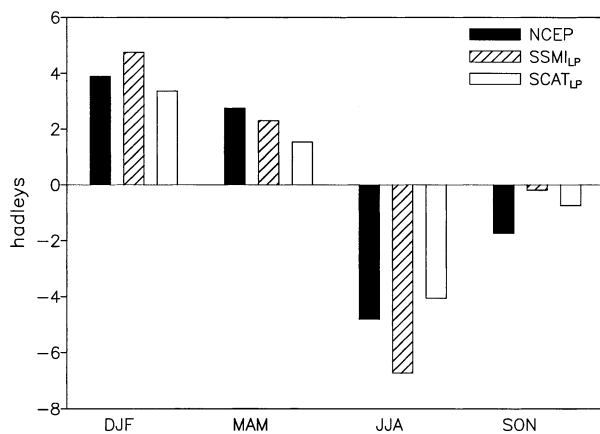

FIG. 3. Seasonal averages of NCEP–NCAR, SSMI$_{LP}$, and SCAT$_{LP}$ estimates of T_O for the period 1992–99. The x-axis labels denote the three months of each season [e.g., Dec–Jan–Feb (DJF)]. Annual means have been removed.
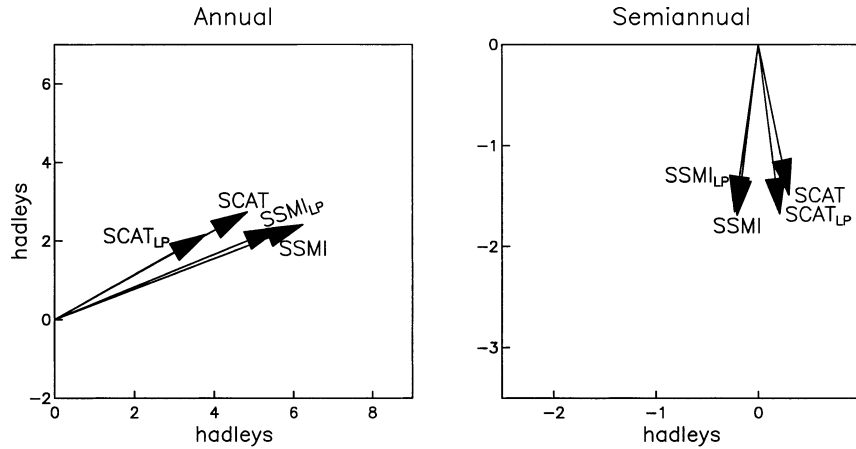
FIG. 4. As in Fig. 1 but for T_O phasors derived from SSMI and SSMI$_{LP}$ series for the period 1994–98, and SCAT and SCAT$_{LP}$ series for the period 1992–99, illustrating the effect of different stress models on T_O.

the respective difference for June–August, which is the season of the largest discrepancy between SSMI$_{LP}$ and NCEP–NCAR torques (Fig. 3). General τ patterns are similar in the two cases, but there are significant differences in amplitude, typically $\sim$0.01–0.02 N m^{-2}, which are not small compared with τ values. Strong disagreements can be seen in the Tropics (e.g., eastern Pacific, Atlantic, and Indian Oceans) and some extratropical southern latitudes. The SSMI$_{LP}$ minus the NCEP–NCAR difference field shows large-scale patterns similar to the original fields, indicative of generally larger amplitudes in the SSMI$_{LP}$ data. In particular, negative values are seen over most of the northern tropics and southern extratropics, where systematically larger negative τ values for SSMI$_{LP}$ are observed. These two latitudinal bands contribute the most to the larger negative SSMI$_{LP}$ values in Fig. 3.

4. Balance between $\dot{M}$ and T revisited

Given the uncertainties suggested by the analysis in section 3, it is useful to assess the extent to which errors in T_O are responsible for seasonal imbalances between $\dot{M}$ and T. We would also like to assess whether any of the T_O time series considered are clearly superior in this regard. Based on (1), our approach is to compare the various T_O estimates to the residual $R = \dot{M} - T_L$ calculated from the NCEP–NCAR reanalysis. Uncertainties in R can also be large, mostly because of issues regarding the calculation of T_L and in particular T_{gw} (Ponte and Rosen 2001). To provide a measure of possible uncertainties in R, Fig. 7 shows the annual and semiannual phasors for residuals calculated with T_{gw} included (denoted by $\tilde{R}$) and without T_{gw} (denoted by $\overline{R}$), together with the various estimates of T_O.
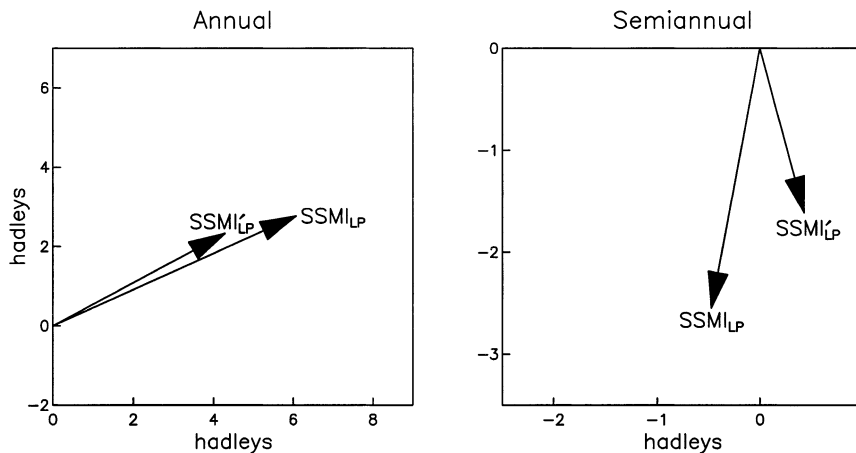

FIG. 5. As in Fig. 1 but for SSMI$_{LP}$ and SSMI$'_{LP}$ series for the period 1992–99, illustrating the effect of temporal resolution of the wind fields on T_O, as described in the text.
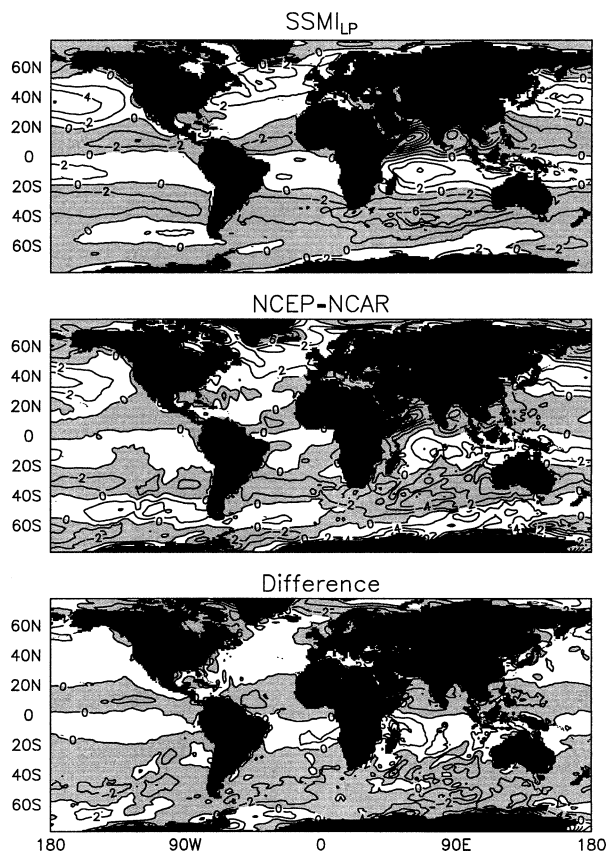
FIG. 6. Estimates of zonal wind stress τ on the atmosphere for JJA season during 1992–99 for SSMI$_{LP}$, NCEP–NCAR, and their difference (SSMI$_{LP}$ minus NCEP–NCAR). Annual means have been removed. Contour interval is 0.02 N m^{-2}. Light shading denotes negative values.

siduals. Differences resulting from the extreme cases of including T_{gw} versus omitting it altogether are taken here as upper bounds on the uncertainties in R, given that other components of T_L are likely to be better determined. Comparing then the uncertainties in R with the spread of T_O estimates in Fig. 7, one concludes that errors in T_O can contribute substantially to the imbalances between $\dot{M}$ and T at the seasonal timescale. Differences in T_O phasors have amplitudes on the order of 1 or 2 hadleys and are ~25% and 100% of the maximum uncertainties in R at annual and semiannual periods, respectively.

The match between $\overline{R}$ (no T_{gw} effect) and all estimates of T_O is poor both in amplitude and phase, with the smallest discrepancies obtained with SCAT$_{LP}$ and SSMI$_{LP}$ for annual and semiannual cycles, respectively. Substantial improvement is obtained, however, when $\tilde{R}$ (T_{gw} effects included) is used. In the latter case, SSMI$_{LP}$ series provide the best match with $\tilde{R}$ both for annual and semiannual periods. Phases of SCAT$_{LP}$ also tend to be in slightly closer agreement than those of NCEP–NCAR; its amplitudes are, however, small, possibly because of the weekly sampling of the SCAT wind fields, as discussed in section 3. Nevertheless, the vector difference between SCAT$_{LP}$ and $\tilde{R}$ is still smaller than that obtained for NCEP–NCAR for the semiannual cycle and very similar for the annual cycle. From this perspective, the use of satellite data generally seems to improve the estimates of T_O over those of NCEP–NCAR, although differences in stress models and effects of using ECMWF winds as background fields in SSMI series may also contribute to the observed differences between NCEP–NCAR and the other two series.

5. Summary and discussion

Our analysis of multiyear T_O time series based on SSM/I and scatterometer wind data quantifies the expected uncertainties in the available estimates of T_O and
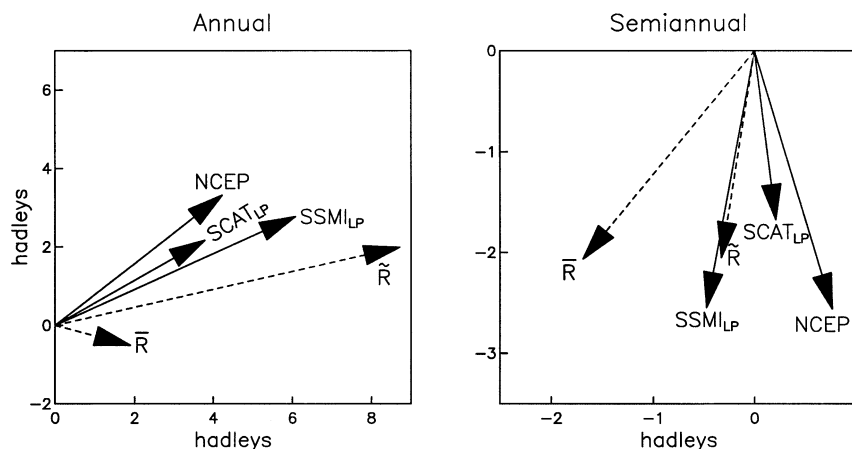
The impact of T_{gw} on R is indeed very large, particularly for the annual cycle. The annual amplitude is much larger when T_{gw} is included, and a change in phase also yields substantial differences in the semiannual re-

FIG. 7. Comparison of the estimates of T_O with the residual $R = \dot{M} - T_L$, calculated for the period 1992–99. Phasor with T_{gw} included is denoted by $\tilde{R}$; phasor without T_{gw} is denoted by $\overline{R}$.

highlights the role of T_O in M budget imbalances at the seasonal timescale. Errors in T_O are directly related to those in the τ fields. The limiting factor in improving the latter seems to be the quality of the input surface winds, rather than the boundary layer models used to infer τ from the winds. Good knowledge of wind variability is needed from seasonal to subweekly timescales. Surface winds over the Tropics and extratropical southern latitudes seem to be currently most uncertain. Examination of the balance between $\dot{M}$ and T suggests that T_O estimates involving satellite winds are generally superior in quality to those based on the NCEP–NCAR reanalysis. A more definite conclusion is hampered, however, by the presence of other large uncertainties in T stemming in part from poor knowledge of T_{gw}.

Ultimately more data will be needed to narrow the uncertainties in the estimates of T_O. We have treated the effects of direct wind field estimates, but other data and methodologies can be used. Such efforts may involve, for example, ocean data assimilation systems that use altimeter (sea level) and other types of data to infer corrections to the surface oceanic forcing fields (including τ) consistent with an improved estimate of the ocean state (Stammer et al. 2002). Preliminary attempts at calculating corrections to T_O in such a way are discussed by Ponte et al. (2001, 2002). More conventionally, the use of satellite surface winds in atmospheric data assimilation systems may also provide for very efficient ways of extracting all the useful information contained in the wind data (e.g., Atlas et al. 2001) and for more accurate determination of T_O.

The importance of subweekly wind variability for seasonal T_O signals raises a set of broader issues. Our finding is a clear example of nonlinearities playing a role in climate variability; that is, synoptic winds can affect the amplitude and phase of seasonal or longer period signals in the oceanic forcing fields and ultimately in the ocean's response. As such, one may need to have very good temporal resolution of variables like near-surface winds for ocean modeling purposes. How fine that resolution may have to be (e.g., is 6-hourly data sufficient for our T_O problem?) is still an unanswered question. In this light, effects of high-frequency noise also become important and will have to be dealt with in tandem.

Finally, we return to the difficulties in finding a good seasonal $\dot{M}$ and T balance and the controversial role of T_{gw}. Results in Fig. 7 indicate that agreement between $\dot{M}$ and T at annual and semiannual periods tends to be better when T_{gw} effects are included. These findings do not contradict those of Huang et al. (1999), who question the quality of T_{gw} values based on the large bias they introduce in the balance between $\dot{M}$ and T in all seasons. Such biases are related to the total value of T_{gw} and thus strongly affected by the large annual mean of T_{gw}. We, in turn, have focused on the torque variability about the annual mean. While questions about the quality of the mean values of T_{gw} remain, our analysis indicates that the variability in T_{gw} is usefully incorporated in seasonal M budgets. In this context, continuing research on the nature of T_{gw} and on improving its parameterization in atmospheric models and analyses is very relevant. Improved estimates of T_O would also help check the quality of future estimates of T_{gw}.

REFERENCES

Atlas, R., S. C. Bloom, R. N. Hoffman, J. V. Ardizzone, and G. Brin, 1991: Space-based surface wind vectors to aid understanding of air–sea interactions. *Eos, Trans. Amer. Geophys. Union,* **72,** 201–208.

——, R. N. Hoffman, S. C. Bloom, J. C. Jusem, and J. Ardizzone, 1996: A multiyear global surface wind velocity dataset using SSM/I wind observations. *Bull. Amer. Meteor. Soc.,* **77,** 869–882.

——, and Coauthors, 2001: The effects of marine winds from scatterometer data on weather analysis and forecasting. *Bull. Amer. Meteor. Soc.,* **82,** 1965–1990.

Boer, G. J., 1990: The earth–atmosphere exchange of angular momentum simulated in a model and implications for the length of day. *J. Geophys. Res.,* **95,** 5511–5531.

Bryan, F. O., 1997: The axial angular momentum balance of a global ocean general circulation model. *Dyn. Atmos.–Oceans,* **25,** 191–216.

CERSAT, 2000: *Mean surface wind fields from the ERS-AM1 and ADEOS-NSCAT microwave scatterometers, August 1991 to May 2000.* WOCE Global Data, Version 2.0, CD-ROM.

Huang, H.-P., and P. D. Sardeshmukh, 2000: Another look at the annual and semiannual cycles of atmospheric angular momentum. *J. Climate,* **13,** 3221–3238.

——, ——, and K. M. Weickmann, 1999: The balance of global angular momentum in a long-term atmospheric data set. *J. Geophys. Res.,* **104,** 2031–2040.

Large, W. G., and S. Pond, 1982: Sensible and latent heat flux measurements over the oceans. *J. Phys. Oceanogr.,* **12,** 464–482.

Lejenäs, H., R. A. Madden, and J. J. Hack, 1997: Global atmospheric angular momentum and earth–atmosphere exchange of angular momentum simulated in a general circulation model. *J. Geophys. Res.,* **102,** 1931–1941.

Liu, W. T., K. B. Katsaros, and J. A. Businger, 1979: Bulk parameterization of air–sea exchanges of heat and water vapor including molecular constraints at the interface. *J. Atmos. Sci.,* **36,** 1722–1735.

Ponte, R. M., and R. D. Rosen, 1993: Determining torques over the ocean and their role in the planetary momentum budget. *J. Geophys. Res.,* **98,** 7317–7325.

——, and ——, 1994: Oceanic angular momentum and torques in a general circulation model. *J. Phys. Oceanogr.,* **24,** 1966–1977.

——, and ——, 1999: Torques responsible for evolution of atmospheric angular momentum during the 1982–83 El Niño. *J. Atmos. Sci.,* **56,** 3457–3462.

——, and ——, 2001: Atmospheric torques on land and ocean and implications for Earth's angular momentum budget. *J. Geophys. Res.,* **106,** 11 793–11 799.

——, D. Stammer, and C. Wunsch, 2001: Improving ocean angular momentum estimates using a model constrained by data. *Geophys. Res. Lett.,* **28,** 1775–1778.

——, A. Mahadevan, J. Rajamony, and R. D. Rosen, 2002: Effects of SSM/I winds on stress torques over the ocean and the atmospheric angular momentum balance. *Proc. WCRP/SCOR Workshop on Intercomparison and Validation of Ocean–Atmosphere Flux Fields,* WCRP-115, WMO/TD-1083, Potomac, MD, WCRP, 99–102.

Rosen, R. D., 1993: The axial momentum balance of Earth and its fluid envelope. *Surv. Geophys.,* **14,** 1–29.

——, D. A. Salstein, and T. M. Wood, 1991: Zonal contributions to global momentum variations on intraseasonal through interannual timescales. *J. Geophys. Res.,* **96,** 5145–5151.

Salstein, D. A., K. Cady-Pereira, C.-K. Shum, and J. Xu, 1996: *ERS-1* scatterometer observations of ocean surface winds as applied to the study of the Earth's momentum balance. Preprints, *Eighth Conf. on Satellite Meteorology and Oceanography,* Atlanta, GA, Amer. Meteor. Soc., 439–442.

Smith, S. D., 1988: Coefficients for sea surface wind stress, heat flux, and wind profiles as a function of wind speed and temperature. *J. Geophys. Res.,* **93,** 15 467–15 472.

Stammer, D., and Coauthors, 2002: Global ocean circulation during 1992–1997, estimated from ocean observations and a general circulation model. *J. Geophys. Res.,* **107** (C9), 3118, doi: 10.1029/2001JC000888.

Wahr, J. M., and A. H. Oort, 1984: Friction- and mountain-torque estimates from global atmospheric data. *J. Atmos. Sci.,* **41,** 190–204.

White, R. M., 1949: The role of the mountains in the angular momentum balance of the atmosphere. *J. Meteor.,* **6,** 353–355.

Widger, W. K., 1949: A study of the flow of angular momentum in the atmosphere. *J. Meteor.,* **6,** 291–299.

Xu, J., 1997: Application of satellite scatterometer to the study of Earth angular momentum balance. Ph.D. dissertation, University of Texas at Austin, 181 pp.